The Biophysicist

Translating DNA Origami Nanotechnology to Middle School, High School, and Undergraduate Laboratories

Peter E. Beshay[1,§], Anjelica Kucinic[2,§], Nicholas Wile[3], Patrick Halley[1], Lilly Des Rosiers[4], Amjad Chowdhury[2], Julia L. Hall[5], Carlos E. Castro[1,6,*], Michael W. Hudoba[3,*]

[1]Department of Mechanical and Aerospace Engineering, Ohio State University, Columbus, OH, USA
[2]Department of Chemical and Biomolecular Engineering, Ohio State University, Columbus, OH, USA
[3]Department of Engineering, Otterbein University, Westerville, OH, USA
[4]Department of Civil, Environmental, and Geodectic Engineering, Ohio State University, Columbus, OH, USA
[5]Mifflin High School, Columbus, OH, USA
[6]Biophysics Graduate Program, Ohio State University, Columbus, OH, USA

ABSTRACT DNA origami is a rapidly emerging nanotechnology that enables researchers to create nanostructures with unprecedented geometric precision that have tremendous potential to advance a variety of fields, including molecular sensing, robotics, and nanomedicine. Hence, many students could benefit from exposure to basic knowledge of DNA origami nanotechnology. However, due to the complexity of design, cost of materials, and cost of equipment, experiments with DNA origami have been limited mainly to research institutions in graduate-level laboratories with significant prior expertise and well-equipped laboratories. This work focuses on overcoming critical barriers to translating DNA origami methods to educational laboratory settings. In particular, we present a streamlined protocol for fabrication and analysis of DNA origami nanostructures that can be carried out within a 2-h laboratory course using low-cost equipment, much of which is readily available in educational laboratories and science classrooms. We focus this educational experiment module on a DNA origami nanorod structure that was previously developed for drug delivery applications. In addition to fabricating nanostructures, we demonstrate a protocol for students to analyze structures via gel electrophoresis using classroom-ready gel equipment. These results establish a basis to expose students to DNA origami nanotechnology and can enable or reinforce valuable learning milestones in fields such as biomaterials, biological engineering, and nanomedicine. Furthermore, introducing students to DNA nanotechnology and related fields can also have the potential to increase interest and future involvement by young students.

KEY WORDS first-year undergraduate/general; high school laboratories; interdisciplinary/multidisciplinary; hands-on learning/manipulatives; biotechnology; DNA nanotechnology

"*"co–corresponding authors

"§"co–first authors

Received: 24 October 2022
Accepted: 7 February 2023
Published: 9 May 2023

I. INTRODUCTION

DNA origami is a rapidly emerging technology that has demonstrated tremendous promise for applications including molecular sensing, nanorobotics, and nanomedicine (1–5). In this approach, a long single-stranded DNA (ssDNA) "scaffold" strand is folded into a

compact structure via DNA base-pairing interactions with many shorter ssDNA "staple" strands, allowing researchers to create nanostructures with unprecedented geometric precision via molecular self-assembly (6–8). Due to the complexity of design and the cost of materials and equipment, DNA origami studies have been limited mainly to research institutions in graduate-level laboratories with significant prior expertise and well-equipped laboratories. However, many students can benefit from exposure to and basic knowledge of DNA origami nanotechnology since it is likely to impact a wide range of fields and industries. Furthermore, DNA origami can serve as an introduction to more general biomolecular engineering concepts, and given the wide range of functions that have been implemented in DNA design, such as mechanical deformation (9), polymerization (10), actuation (11) and so on, DNA nanotechnology can be a unique way to introduce or reinforce other science and engineering concepts. Over the long term, introducing a broad range of students to DNA origami would also have the potential to advance the field due to increased interest and involvement by young students, who may then pursue education, research, or career paths related to DNA nanotechnology (12).

We believe that by circumventing the complexity of the design process and removing the hefty cost and infrastructure associated with DNA origami fabrication, valuable educational milestones can be achieved by young students in fields such as engineering, chemistry, physics, biology, materials science, medicine, and computer science. For example, specific learning opportunities that lie in DNA nanostructure fabrication include topics such as charge screening, mechanical deformations, conformational dynamics and free energy landscapes, nanoscale stimulus response, polymerization, and algorithmic design and assembly (13–18). However, current DNA origami methods are not suitable for translation to classrooms, even for well-equipped instructional laboratories. DNA origami development often requires days or up to several weeks of design and optimization (19–21). Furthermore, fabrication typically takes many hours or days and is carried out on costly polymerase chain reaction thermocyclers (19, 22), while the analysis of structure folding and behavior can take several hours with the most common first step of analysis carried out using laboratory gel electrophoresis equipment (19, 23). These demands leave these topics out of reach for most undergraduate and high school educational laboratories and middle school science rooms.

To facilitate educational translation of DNA origami methods, here we developed a streamlined approach to introduce and carry out DNA origami fabrication in educational laboratories or classrooms with equipment that is either readily available or relatively inexpensive. The entire streamlined fabrication and analysis process can be carried out within a 2-h lab session or in 1 h with additional teacher preparation, making it viable to carry out in standard laboratory class periods. We present a specific laboratory module based on a previously published DNA origami nanostructure (3, 24) that introduces the concept and importance of charge screening during the folding process of a DNA origami nanodevice. We anticipate that this work can open a door to introducing DNA origami to undergraduate, secondary, and primary school students and serve as a foundational example to stimulate additional educational translation related to DNA origami nanotechnology.

A. DNA origami: design, fabrication, and analysis overview

The year 2022 marked the 40th anniversary of the original conception of making synthetic nanostructures out of DNA with the idea of building 2- or 3-dimensional lattices out of many similar copies of nucleic acid junctions (25). In 2006, the development of scaffolded DNA origami (6), which we refer to here as just DNA origami, took a major step in enabling more complex nanostructure geometries with a robust and versatile design and fabrication process. DNA origami is based on folding a long scaffold strand, typically ~7000 to 8000

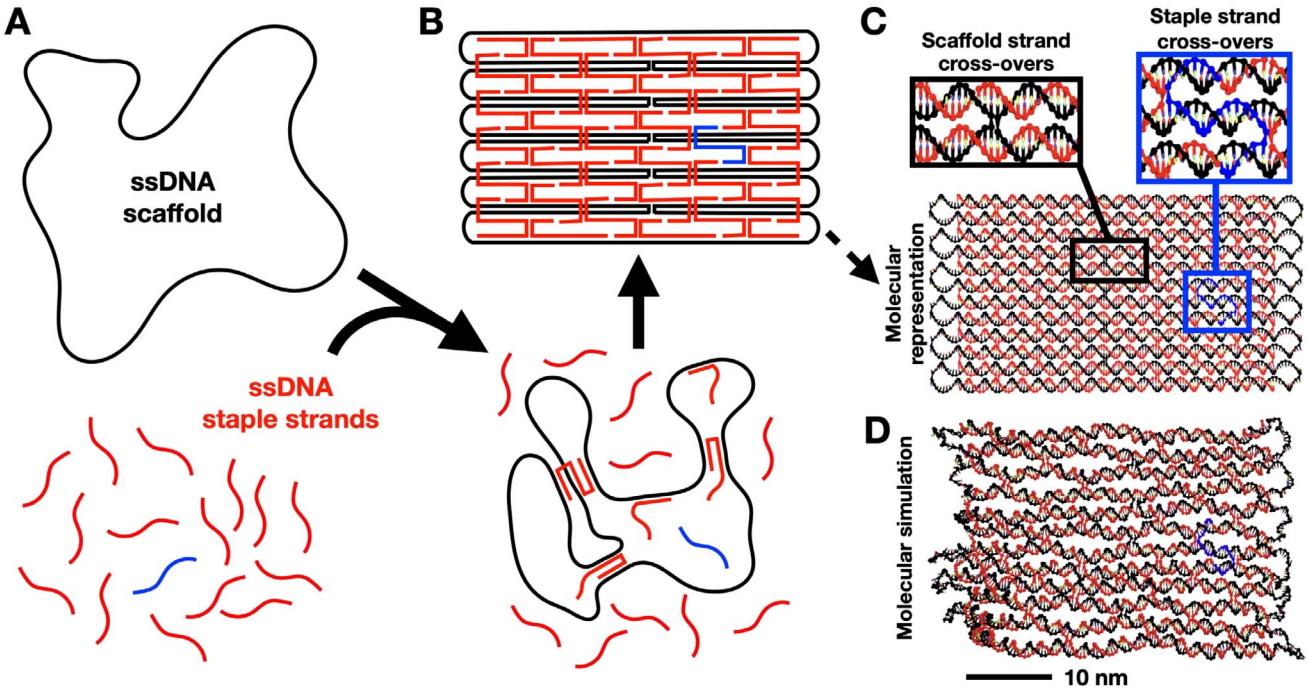

Fig 1. DNA origami self-assembly. (A) A long (usually thousands of nucleotides) ssDNA scaffold is folded into a compact structure via base-pairing interactions with many ssDNA staple strands. The staple strands are designed to be piecewise complementary to the scaffold so that they "pinch" or fold the scaffold into the target shape. (B) A schematic scaffold and staple strand routing design illustrates how the staples collectively hold the scaffold in the target shape, in this case an example of a rectangular plate design. Each staple, for example, the blue strand, is incorporated at a specific location based on its sequence. (C) A molecular model shows how the DNA helical geometry enables crossover connections between neighboring helices. (D) A coarse-grained molecular dynamics simulation with the oxDNA model illustrates a more realistic depiction of the DNA origami rectangular plate design.

nucleotides long, into a compact nanostructure through Watson-Crick base-pairing interactions (26–28) with many, often ∼150 to 200, shorter staple strands that are ∼30 to 50 nucleotides long. The staple strands are designed to be piecewise complementary to the scaffold so that binding pinches, or folds (hence the term "origami"), the scaffold into the desired shape (Fig 1A,B). Those shapes typically consist of several double-stranded DNA (dsDNA) helices connected in parallel into bundles with a prescribed geometry where helices are connected to their neighbors at regular intervals by junctions, similar to Holliday junctions (29, 30), where scaffold or staples cross from one helix to the neighboring one (Fig 1C,D). This approach allows for the fabrication of precise nanostructures with dimensions on the 5-to-100-nm scale and unprecedented geometric complexity. Examples include 100-nm-wide smiley faces (6), intricate ∼5- to 100-nm wireframe structures (31, 32), dynamic components like hinges (13, 33), sliders (33, 34), rotors (35, 36), or even ∼150-nm airplanes (21). Here we focused our development of classroom methods for DNA origami fabrication on a previously designed nanorod structure that is in development as a drug delivery device (3). The device is referred to as the "Horse," as in the original publication, inspired by the concept of the Trojan Horse.

The basic DNA origami nanostructure design process (20) follows several common steps: (a) defining the geometry (i.e., cross section in terms of dsDNA helices and the lengths of those helices), (b) scaffold routing, (c) staple routing, and (d) staple sequence determination. These steps are typically carried out using custom computer-aided design (CAD) software. The most widely used software since the development of DNA origami is caDNAno37, and a number of more recent tools have led to faster, partially or fully automated, and more advanced design capabilities (21, 32, 38–40). In

addition, significant research over the past decade has led to a number of simulation tools (19, 41–44) that are useful to predict the structure of DNA origami. Figure 1D illustrates a molecular simulation for the small DNA origami rectangular plate example simulated using the oxDNA coarse-grained molecular dynamics model (41, 42). The DNA origami structure of interest for this work, the Horse nanostructure, was designed in the software caDNAno37. Although we circumvent the design process in our educational translation by using a previously published device, this work can still serve as a basis for introducing and learning the DNA origami design process. To facilitate that, we provided a schematic of the Horse structure caDNAno design in Figure S1.

Once the staples are designed, they are typically ordered from one of several commercial vendors who synthesize custom DNA oligonucleotides, and the scaffold can also be purchased from a commercial vendor or produced in a laboratory as previously described (19). Once the scaffold and staples are obtained, the fabrication, or folding, of DNA origami structures is carried out via a temperature-controlled molecular self-assembly process. Commonly used fabrication protocols are described in detail here (19, 23, 45). To fold the structure, the combination of staples strands is mixed in 10-fold excess relative to the scaffold strand, and the mixture is subjected to a thermal folding ramp that consists of 3 phases: a melting phase, an annealing phase, and a cooling phase. Details can vary from structure to structure and are often subject to optimization for individual structures. Generally, the thermal annealing can take many hours or up to several days. For the case of the Horse nanostructure, the original fabrication thermal ramp consisted of melting at 65 °C for 10 min, followed by slow cooling from 60 °C to 25 °C over the course of 17 h, and finally rapid cooling to 4 °C (3).

After fabrication, a common first-step assay to evaluate folding is agarose gel electrophoresis (19). The well-folded compact structures typically migrate through the gel faster than misfolded structures. In most (but not all) cases, the compact folded structure also runs faster than the component scaffold strand, which can be included as a reference. A sharp band that migrates on the gel faster than the scaffold is typically indicative of a well-folded structure. Gel electrophoresis can also serve as a convenient purification approach to separate well-folded from misfolded structures and from excess staple strands. To confirm folding and quantify shape and distributions of conformations, folded structures are subjected to imaging via transmission electron microscopy (TEM) or atomic force microscopy (AFM). Protocols for TEM imaging are provided in the methods and both methods are described in detail here (19, 21, 23, 46).

B. Key barriers to educational translation

This work focuses on eliminating major barriers that make DNA origami fabrication and experiments challenging to perform in educational laboratories and classroom environments. The barriers are related primarily to resources and time required for DNA origami. The first major barrier of resources is due to the equipment needs that range from possibly available (e.g., gel electrophoresis) to unlikely available (e.g., thermocyclers) or impractical (e.g., AFM or TEM) for ready access in educational settings. The barrier of time comes from all stages of the process, including (a) design (designing DNA origami structures can take days to weeks, especially for new designers, and even more recent automated or partially automated tools take time to learn), (b) fabrication (self-assembly reactions can take several hours to prepare and up to days to run the thermal ramps), and (c) analysis (gel electrophoresis typically requires 2 to 3 h to set up and run, and AFM or TEM imaging is likely impractical for most educational settings). In addition to these barriers, the shear complexity of designs and the fabrication process are challenges to educational translation. Here we overcome these barriers to enable the hands-on introduction and use of DNA origami

technology in instructional labs and classrooms.

II. METHODS

A. Folding DNA origami

The horse nanostructures were folded in a single-pot reaction with 200 nM single-stranded DNA oligos (Integrated DNA Technologies), 20 nM M13mp18-derived scaffolds (prepared in-house as described in Castro et al. (19)), 20 mM $MgCl_2$ (unless otherwise noted), and a buffer containing 5 mM Tris, 5 mM NaCl (pH 8), and 1 mM EDTA; 1.5-mL Eppendorf tubes were used for classroom folding experiments, and 200-μL Eppendorf tubes were used for laboratory folding experiments. The respective folding equipment and conditions are described below for the laboratory and classroom protocols.

1. Laboratory folding

The single-pot reaction was placed into a thermocycler (Bio-Rad Laboratories, Hercules, CA) first at 65 °C for 5 min to melt the mixture and next to anneal for certain time and temperature points as described in the results and discussion in the main text. The mixture was then cooled to 4 °C and placed into a refrigerator until purification and further analysis.

2. Classroom folding

The single-pot reaction was placed in a water bath at 65 °C for 5 min for a melting phase, then exposed to a water bath at 52.5 °C ± 0.5 °C for different time points as described in the results and discussion in the main text. The mixture was then cooled in an ice bath until purification.

B. Purification of DNA origami

DNA origami Horse nanostructures were purified via agarose gel electrophoresis using the respective gel electrophoresis kit for the laboratory or classroom as described below.

1. Laboratory purification

Folded DNA origami nanostructures were purified via an Owl EasyCast B1 mini gel electrophoresis kit (Thermo Fisher Scientific, Waltham, MA). For the EasyCast gel, 140 mL of running buffer was created by mixing 7 mL of 10× (Tris/Borate/EDTA [TBE] buffer containing 45 mM boric acid, 45 mM Tris(hydroxymethyl)-aminomethane base, and 1 mM (ethylenedinitrilo)tetraacetic acid), 611 μL of 1.375 M $MgCl_2$, and 132.4 mL of double-distilled water. The gel was cast by microwaving 0.62 g of agarose with 61.8 g of distilled water. Once the agarose is dissolved and evaporated water is replaced, 250 μL of 1.375 M $MgCl_2$ and 3 μL of SYBR safe or 0.5 μg mL/L ethidium bromide DNA stain was mixed. The gel was then poured and allowed to solidify; 15 μL of folded Horse structure and 3 μL of blue loading dye were pipetted into the wells of the solidified gel. Running buffer was poured into the gel rig, and the gel was run at 90 V for 90 min in an ice water bath. The gel was then imaged on an ultraviolet light table.

2. Classroom purification

Folded DNA origami nanostructures are purified via the MiniOne agarose gel electrophoresis kit. For the MiniOne gel, 140 mL of running buffer was created by mixing 7 mL 10× TBE, 300 μL of 1.375 M $MgCl_2$, and 132.7 mL of distilled water. Next, the gel was cast by microwaving 0.5 g agarose with 49.6 g distilled water. After dissolving the agarose and replacing any evaporated water, 109 μL of 1.375 M $MgCl_2$, and 4 μL of GelGreen DNA stain was mixed. The gel was then poured and allowed to solidify; 8 μL of folded Horse structure and 2 μL of orange loading dye were pipetted into the wells of the solidified gel. Running buffer was poured into the MiniOne gel rig, and the gel was run for 30 to 40 min at 42 V. The gel is imaged via the blue light equipped in the MiniOne gel rig with a cell phone.

C. Imaging DNA origami

Purified DNA origami Horse nanostructures were suspended in the respective running buffer conditions post-gel electrophoresis at concentrations between 1 and 5 nM. A 4-μL sample droplet was deposited onto a plasma-treated Formvar-coated 400-mesh copper grid (Ted Pella) and incubated for 4 min. The droplet was wicked away on filter paper; afterward, the grid picked up a 10-μL droplet of staining solution

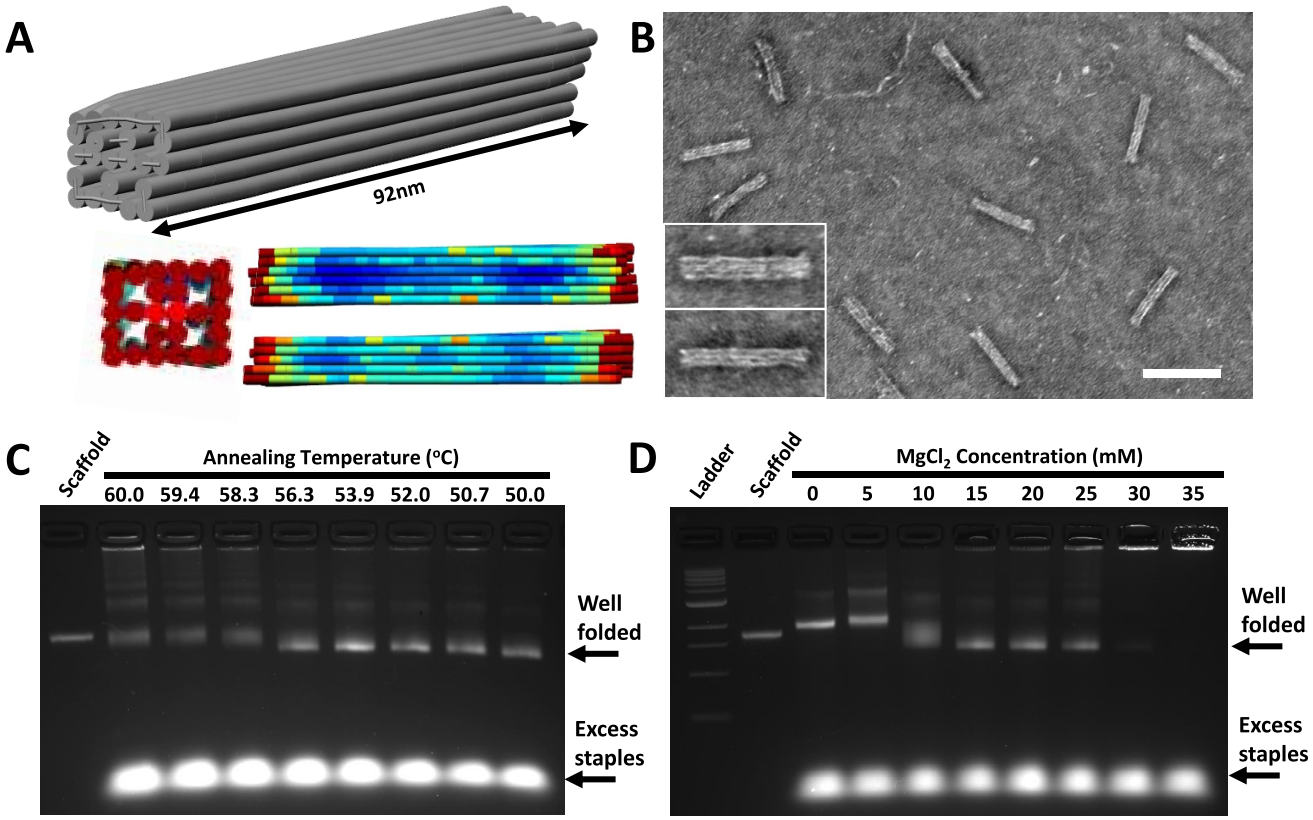

Fig 2. DNA origami "Horse" nanorod structure design and fabrication. (A) Models of the Horse nanostructure simulated using Cando46. The color scale illustrates relative magnitude of root-mean-squared fluctuations. (B) Transmission electron microscopy image of the Horse (scale bar = 100 nm) folded at 20 mM $MgCl_2$ in a 15-min thermal ramp with 5 min at 65 °C, 15 min at 52 °C, and 5 min at 4 °C. Insets show zoomed in views of top and side views of the Horse nanostructure. (C) Agarose gel electrophoresis (AGE) analysis of nanostructures folded in a thermocycler for 10 min at varying annealing temperatures compared with the M13mp18 scaffold. The gel shows well-folded structures over a range of annealing temperatures from 50.0 °C to 56.3 °C that run slightly faster than the scaffold and the excess staples that run much faster than the folded structures. (D) AGE analysis of nanostructures folded in a thermocycler at 52 °C for 10 min with varying concentrations of $MgCl_2$ compared with a 100-kB ladder and scaffold show well-folded structures at $MgCl_2$ concentrations ranging from 15 to 25 mM. Structures are misfolded at 0 to 5 mM (indicated by slower-running bands), partially folded at 10 mM (indicated by slightly slower and smeared band), and aggregate at 30 to 35 mM (indicated by bright signal stuck in the well).

containing 2% uranyl formate and 25 mM NaOH and then was immediately wicked away. This was followed by picking up a 20-μL droplet of the same staining solution and incubating for 40 seconds before wicking away on the filter paper. The prepared samples were then dried for at least 20 min before imaging. The structures were imaged at the Ohio State University Campus Microscopy and Imaging Facility on a FEI Tecnai G2 Spirit TEM at 80-kV acceleration.

III. RESULTS AND DISCUSSION

A. DNA origami design

Designing structures using caDNAno37 can take days to weeks, especially for new designers. Recent automated or semiautomated tools allow for design in minutes (21, 32, 38–40). These approaches still require introducing software, which can take several hours to days to present and learn to operate. We circumvent the design process by relying on the previously published Horse nanostructure (3) (Fig 2A). This also allows students to work with a device that is directly relevant to a key application space for DNA origami, namely, drug delivery. While it is not essential for learning the basics of DNA origami fabrication and analysis, which is the focus here, we envision that the design process could be introduced in parallel as desired.

B. Rapid fabrication of DNA origami

The Horse nanostructure fabrication was originally carried out via self-assembly in a thermocycler over the course of ∼17 h. To reduce this time and eliminate the need for costly equipment, we built on recent work demonstrating faster (24, 45) and low-cost (24) methods to fold DNA origami structures. Halley et al. (24) demonstrated that the Horse structure folds well within a range of constant annealing temperatures between 40 °C and 60 °C when annealed for 4 h, and at a particular annealing temperature, the Horse structure can fold in as little as 10 min of annealing. This suggests that folding the Horse structure requires only holding a melting temperature at 65 °C and an annealing temperature at 52 °C, followed by rapid cooling, which could be carried out using equipment such as water baths and ice buckets.

Expanding on this work, we aimed to minimize the folding time without the need for precise temperature control. We tested 2 critical parameters for folding: the annealing temperature and the $MgCl_2$ concentration. The presence of positive ions is essential to screen the repulsions of the negatively charged phosphate groups on the DNA strands (i.e., charge screening), and temperature regulates the stability of binding interactions between the staples and scaffold, allowing the strands to bind in the most stable configuration. We tested these parameters with a rapid thermal cycle consisting of 5 min at 65 °C, 10 min at a constant annealing temperature (performed in a laboratory thermocycler), followed by rapid cooling to 4 °C. We first tested a range of constant annealing temperatures from 60 °C to 50 °C using a $MgCl_2$ concentration of 20 mM, which leads to high yield assembly for longer annealing times (24). The folding results were analyzed by TEM (Fig 2B) and agarose gel electrophoresis (AGE), performed with laboratory AGE equipment (Fig 2C). These results show that with this ∼15-min folding protocol, the structures fold at annealing temperatures in the range of 50 °C to 56 °C, with 56 °C showing a decreased yield as indicated by the slightly smeared band. These results suggest that the Horse nanostructure folds in ∼15 min with the highest yields observed in the 50 °C-to-54 °C annealing temperature range.

We also investigated how the ∼15-min folding is affected by varying $MgCl_2$ concentrations, both to confirm that 20 mM $MgCl_2$ remains an optimal concentration and as a precursor to the intended laboratory experiment module, which focuses on introducing the concept of screening salt concentrations as a common optimization step for DNA origami fabrication. Horse nanostructures were folded in a laboratory thermocycler at 52 °C with the same ∼15-min thermal cycle, and $MgCl_2$ concentrations varied from 0 to 35 mM $MgCl_2$ in 5-mM increments. AGE results (Fig 2D) show that structures begin to form at 10 mM $MgCl_2$ and fold most efficiently at 15 to 20 mM $MgCl_2$. At 25 mM and above, structures exhibit increasing aggregation, indicated by the build-up of signal in the wells since large aggregates cannot migrate into the gel.

For both sets of experiments, we confirmed that the leading bands consisted of well-folded Horse nanostructures by TEM imaging. Figure 1B shows a representative TEM image of Horse nanostructures folded at 20 mM $MgCl_2$ using the ∼15-min folding protocol with annealing at 52 °C, depicting well-folded structures. Combined, these results show that Horse structures can fold with high yield within ∼15 min at 20 mM $MgCl_2$, including 10 min of annealing at temperatures in the range of 50 °C to 54 °C. While we used 65 °C for melting here, prior work has used up to 95 °C for the melting phase (6, 7), suggesting that precise control of the melting temperature is also not critical.

C. Rapid fabrication of DNA origami with classroom-ready equipment

We aimed to translate this fast and simple folding approach to classroom-ready equipment. Building on Halley et al. (24), who demonstrated DNA origami folding with heated water baths, we developed a folding approach that utilizes 2 hot plates to heat 2 1-L beakers filled with ∼500 mL of water (i.e., water baths) and an ice bucket (or additional beaker) filled with ice and water. The heated

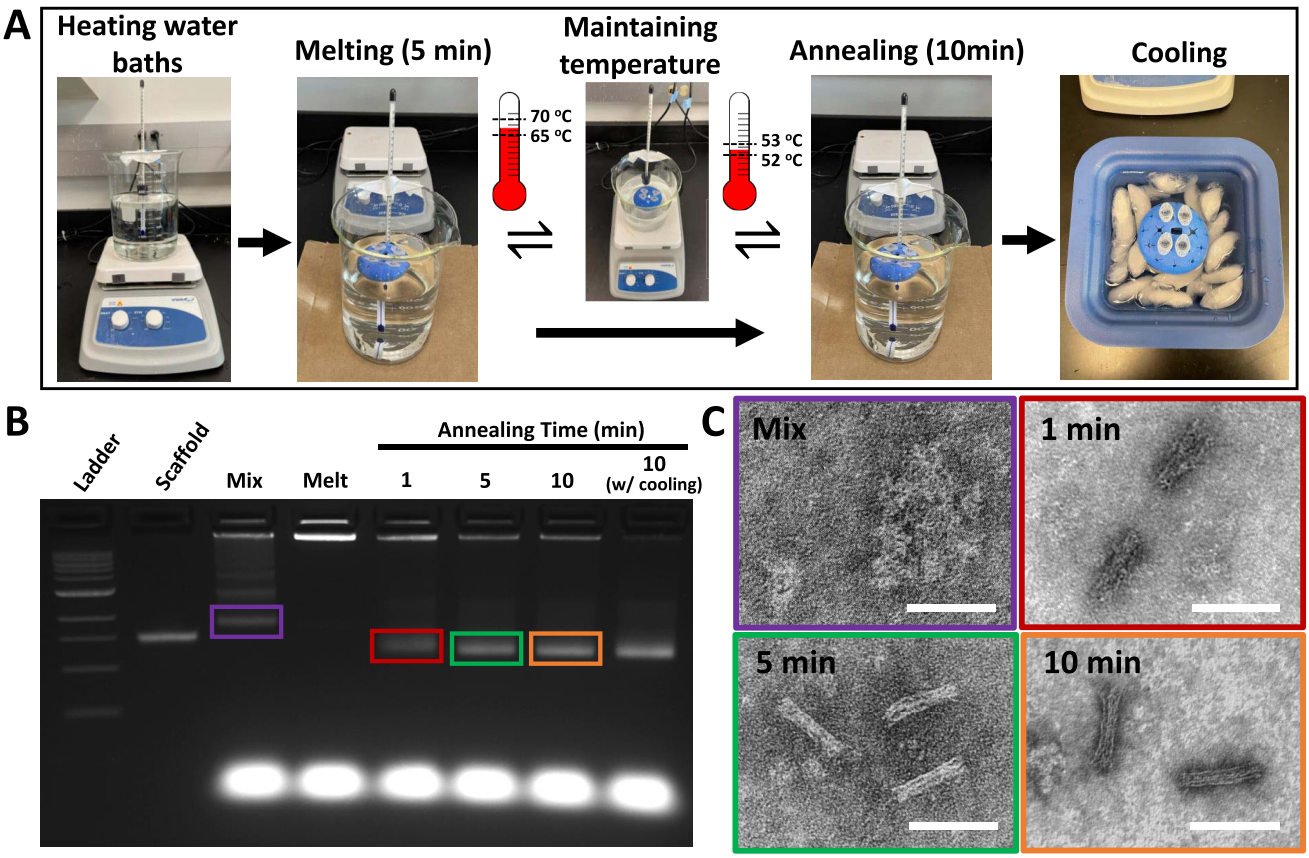

Fig 3. Classroom-ready fabrication of DNA origami Horse nanostructures. (A) Two water baths are prepared with 500 mL of water in a 1-L beaker. One for melting is maintained at temperatures in the range of 65 °C to 70 °C and the other at the proper annealing temperature, which is 52 °C to 53 °C for the Horse structure. Temperatures are monitored with thermometers directly in the heated water baths. The beakers are removed from the hot plate and placed on the lab bench on top of cardboard (for insulation) when reaching the upper limit of the temperature range and placed back on the hot plate when reaching the lower limit of the target temperature range. Folding reactions in small tubes containing DNA scaffold and staple strands are placed in the melting beaker for 5 min and then in the annealing beaker for 10 min and finally cooled in an ice bath for 5 min. After the mixing stage and melting stage and after 1, 5, or 10 min of folding, the solutions were rapidly quenched in liquid nitrogen and then thawed and subjected to (B) agarose gel electrophoresis and (C) transmission electron microscopy analysis to illustrate the progression of the fabrication process. These results illustrate that structures form misfolded "blobs" of DNA on mixing. The melt phase shows aggregated DNA, which may have occurred in sample handling prior to loading the gel. Structures are already mostly folded by 1 min of annealing and fold completely at 5 and 10 min of annealing. The final 10-min lane on the gel was cooled in an ice bath (scale bars = 100 nm).

water baths were used to hold a melting temperature of ~65 °C to 70 °C and an annealing temperature of 52 °C to 53 °C, and the ice bucket was used for the final cooling step. Temperatures were monitored using standard laboratory thermometers placed in each water bath. Rather than seeking specific hot plate settings to achieve the correct temperatures, we established a simpler approach that relies on manual control of the temperatures (Fig 3A). Both hot plates were kept on their high (500 °C) setting, and beakers were placed on the hot plate until the water baths reached the desired temperature range. The beakers were then removed from the hot plate when they reached the target temperature range and placed on the lab bench on a piece of cardboard (for some insulation). Beakers were placed back onto the hot plate when they reached the lower end of the target temperature range. With our experimental setup, we determined that placing the beaker back onto the hot plate for 2 to 3 s on the high setting would raise 500 mL of water by about 1 °C. This manual back-and-forth process between the hot plate and the cardboard was

used during the duration of the 5-min melting and 10-min annealing steps.

Horse nanostructure fabrication was carried out by putting the tube containing the folding reaction solution into the melt water bath for 5 min while it was kept in the target temperature range. Tubes were placed into water baths using foam tube holders thin enough to keep the liquid inside the tube submerged below the water level (Fig 3A). After 5 min, the tubes were moved to the annealing water bath for 10 min while it was held in the desired temperature range. Once 10 min had elapsed, the tubes were transferred to an ice bath for ∼5 min. To reveal better insight into this classroom-ready rapid folding approach, we assessed the folding reaction at several stages during the process—after mixing at room temperature, after the melting phase, and after various annealing times—by assessing a small volume of the folding reaction solution with AGE (Fig 3B) and TEM (Fig 3C). Melt and annealing stage samples were quenched in liquid nitrogen to "flash freeze" the reaction and loaded into gels directly after thawing. TEM images were then taken using gel-purified samples. AGE revealed slower-migrating DNA constructs after mixing, likely due to the scaffold binding staples without forming any well-defined structure, and DNA appeared to be aggregated at the end of the melt phase (stuck in the well), although this may have occurred during sample handling. Both AGE and TEM revealed the basic shape (although not well-defined) folds even with 1 min of annealing, and both 5 and 10 min of annealing led to well-folded structures, which is consistent with prior results (24).

D. Analysis of DNA origami folding using classroom-ready equipment

Traditional laboratory electrophoresis equipment is expensive (∼$1000 to $3000 for a gel rig, including required power supply and light source for visualization), making it impractical for many K-through-12 or undergraduate-level science classrooms. To facilitate broader access, especially for education, some companies have developed inexpensive, safe, and portable gel electrophoresis systems. Here we implemented the MiniOne gel electrophoresis system designed for classroom use (47), which contains a gel rig, power supply, and light source all in 1 compact system at significantly lower cost (<$300 kit; also includes a 20-μL pipette and gel casting equipment). Figure 4A,B compares the equipment needed to set up and run AGE using the MiniOne and research laboratory equipment, respectively.

To test the MiniOne electrophoresis system for DNA origami analysis, we performed a salt screen (similar to Fig 2D) using the previously described ∼15-min hot plate water bath folding approach. Since the MiniOne gels contain 6 lanes, we condensed our salt screen to include folding reactions carried out with 0, 10, 20, and 30 mM $MgCl_2$, leaving room to run a DNA ladder and the ssDNA scaffold as references on the gel. This also conserves materials, which may be an important consideration for educational implementation. The results of these reactions were analyzed by AGE (Fig 4C,D). The MiniOne, however, is designed to run AGE experiments for standard DNA analyses (i.e., not analysis of DNA origami), which are run differently than those typically used for running AGE with DNA origami. DNA origami structures are typically run on 2% agarose gels in a buffer containing 11 mM $MgCl_2$, both in the gel and in the surrounding running buffer, because positive counterions maintain the stability of DNA origami nanostructures. However, we found that the MiniOne system could not run with these conditions, likely due to the excessive current generated from the high concentration of ions, which tends to heat the gel and running buffer. This heating is normally accounted for by cooling the gels in an ice water bath while they run, but this is not practical in the MiniOne system. We tested a series of AGE conditions to converge to a protocol that was compatible with the MiniOne system, maintained DNA origami stability, and enabled visualization of gel shifts indicative of changes on DNA origami folding quality. The resulting AGE-altered conditions consisted of a 1% agarose gel with 3 mM $MgCl_2$ in the gel and running buffer. Importantly, the MiniOne gel

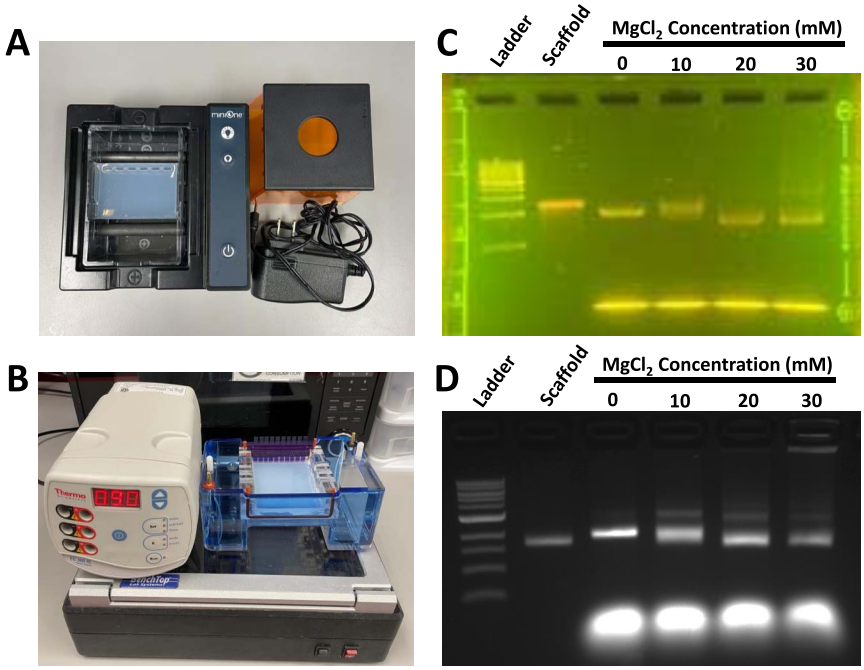

Fig 4. Gel electrophoresis setups using (A) the MiniOne and (B) research laboratory equipment. Agarose gel electrophoresis (AGE) analysis of the folding reactions using varying levels of $MgCl^2$ run alongside a 1-kB ladder and the scaffold for (C) the MiniOne and (D) research laboratory equipment. Gel shifts illustrate expected results where nanostructures are misfolded at 0 to 10 mM, well folded at 20 mM, and begin to aggregate at 30 mM.

kits use GelGreen stain for DNA staining, reducing the risks of exposure to the standard mutagenic stain, ethidium bromide, and harmful UV light exposure.

Figures 4C,D compares AGE analysis of the salt screen on the MiniOne setup and laboratory gel equipment, respectively. Both gels illustrate that 0- to 10-mM $MgCl_2$ leads to misfolded structures. The Horse structure folds well at 20 and 30 mM, but 30 mM also leads to some aggregation, as indicated by the trailing smear in the MiniOne gel and the signal in the well on the laboratory equipment gel.

One additional advantage of the MiniOne system is that the gel migration can be viewed in real time since the visualization is performed directly on the same system as opposed to having to transfer the gel to an imager for the laboratory equipment. Figure 5 shows snapshots of the MiniOne salt screen gel taken at 10-min time intervals (40 min is same as Fig 4C). Structures were visualized using the built-in high-energy LED light source of the MiniOne system, and images were acquired using a smartphone camera. These results illustrate that the relevant gel details (gel shifts indicating well-folded structures and aggregation) can be observed after 30 min. We further confirmed these folding results with TEM imaging of structures purified from the MiniOne gel. Figure 5B shows representative TEM images for each $MgCl_2$ concentration, confirming misfolded structures at 0 mM, partially folded structures at 10 mM, and well-folded structures at 20 to 30 mM.

IV. ADAPTATION TO THE CLASSROOM

Time, cost, and complexity are 3 important factors when developing the protocol to perform this experiment in middle school, high school, and undergraduate classrooms. We have shortened the time required to perform the experiments by developing protocols that can be completed in ~2-h, or 2 1-h, sessions. Alternatively, these experiments could be performed in a shorter ~1-h single session with additional instructor setup and preparation (casting of gels, bringing water baths up to

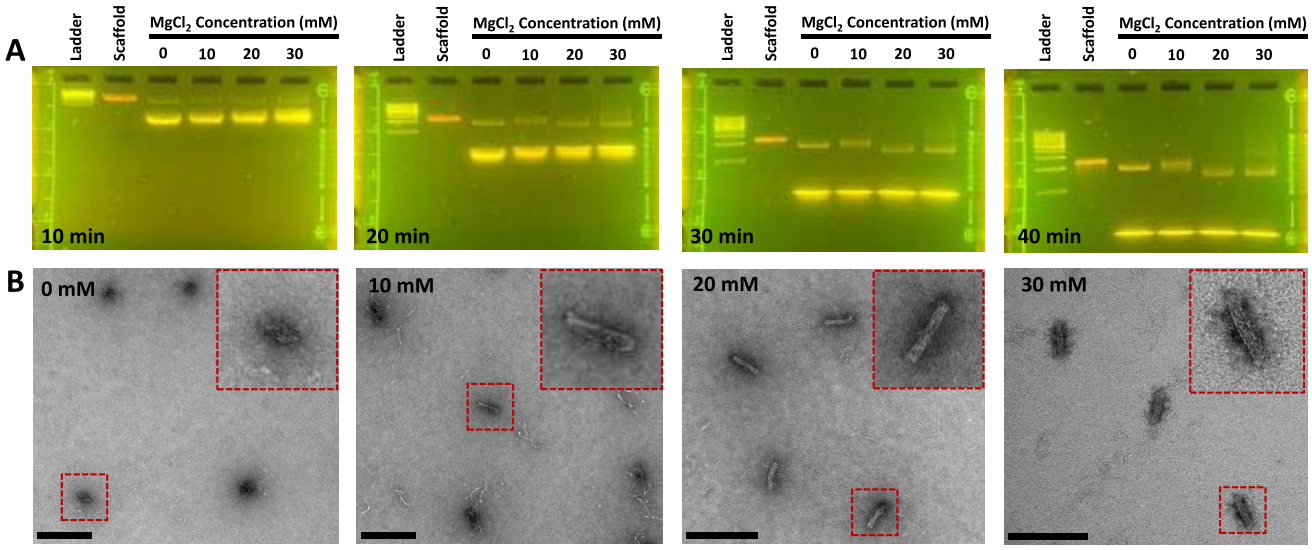

Fig 5. DNA origami classroom AGE analysis of $MgCl_2$ salt screen. (A) Agarose gel electrophoresis (AGE) analysis of Horse nanostructures folded at several $MgCl_2$ concentrations was carried out on the MiniOne system and imaged at several time points. The relevant gel shifts indicating proper folding at 20 mM and aggregation at 30 mM are noticeable by 30 min and clearly visible by 40 min. This MiniOne AGE salt screen represents a folding analysis that can be carried out in a classroom. (B) Transmission electron microscopy images of sample purified from the MiniOne gels confirm poor folding at 0 mM, partial folding at 10 mM, and high-quality folding at 20 to 30 mM (scale bars = 200 nm).

temperature, premixing components of folding reactions, and so on). We also reduced costs by eliminating the need for specialized equipment, including the thermocycler (∼$5000 to $10,000) and laboratory gel electrophoresis equipment (∼$1000 to $2000), UV table and imager (∼$5000 to $10,000) and replacing these with simpler, cheaper, and possibly readily available equipment consisting of hot plates (∼$200 to $300 if not available), glassware (∼$20 per beaker, 2 needed), and the MiniOne gel electrophoresis system (∼$300). A detailed cost comparison with specific examples is provided in Supplemental Table 1. We also significantly reduced complexity by streamlining the folding and analysis process and using the compact classroom-ready equipment.

Here we lay out a proposed procedure for an ∼2-h experiment module for classroom implementation of the DNA origami salt screen presented in Figure 4A. The procedure consisted of 3 main steps: (a) preparing the gel for electrophoresis, (b) running the folding reaction, and (c) running the gel. Each step entails preparation time (which will vary based on the students' prior experience with lab work, pipetting and measuring reagents), and each step has a rate-limiting step (described below).

A. Step 1: preparing the gel for electrophoresis (∼35 min)

Students will prepare the gel running buffer and cast the gel. This involves both standard laboratory measurements as well as pipetting. Preparing the gel takes approximately 15 min. The rate-limiting step here is waiting for the gel to solidify, which takes ∼30 min at room temperature. Students can prepare the folding reaction or bring water baths up to target temperatures while waiting for the gel to solidify.

B. Step 2: running the folding reaction (∼30 min)

In this step, students will prepare the 2 water baths (bringing them to the desired target temperature range), mix the folding reaction, and perform the folding thermal cycle. Students will need to calculate appropriate dilutions to make the different 10× concentrations of a salt buffer (0, 100, 200, and 300 mM $MgCl_2$) and then mix the 5 ingredients at proper volumes and concentrations (scaffold, staple

strands, folding buffer, salt buffer, and water). This process takes ∼15 to 20 min. The rate-limiting step is folding the structure for 20 min (5-min melt, 10-min fold, and 5-min cooling).

C. Step 3: running the gel (∼50 min)

Here, students will perform gel electrophoresis by setting up the gel equipment, mixing the folded structure solution with gel loading dye, loading the samples into wells, and running the gels. Preparation takes ∼10 min, and running the gel takes 30 to 40 min to visualize the gel shift results. Students will compare their results to expected results shown in Figure 4C or D, depending on the electrophoresis setup being used.

The total protocol can be completed in a single, 2-h lab session. If broken up into 2 1-h sessions, the initial session would consist of step 1 and the preparation for step 2 (i.e., mixing folding reactions). The second session would then include running the folding reaction from step 2 as well as running the gel in step 3. Part of the preparation of step 3 (i.e., preparing loading dye) can be done during the folding reaction as long as students can also carefully monitor the water bath temperatures simultaneously. The protocol can also be completed in a single 1-h session if the instructor prepares the gel, water baths, and folding reaction mixtures ahead of time. Students would then perform the folding reaction, mix with loading dye, load, and then run the gel for ∼30 min. This shorter method would be ideal for younger students or students with no prior lab experience.

Table 1 shows the equipment and reagents needed to complete the entire procedure. Many items on the equipment/supplies list (E1 through E12) are commonly found in classroom science laboratories or can be purchased at low cost. E13 through E15 are not as common; however, inexpensive classroom versions exist, such as the MiniOne Gel Electrophoresis Kit used in this research (<$300).

The reagents R1 and R2 are readily found in science laboratories. R3 through R7 can also be purchased at low cost individually or in kits (in these experiments, reagents R3 through R7 were purchased from MiniOne). The reagents R8 through R10 can be provided in small quantities for those interested in performing the procedure.

V. CONCLUSION

In this work, we developed a classroom-ready approach to folding DNA origami nanostructures, and we demonstrated a protocol to perform an experiment that analyzes the effect of salt concentration on DNA origami folding, which is a common first step in optimizing fabrication. These procedures can be done in a time- and cost-effective manner, and variation in complexity allows this to be a valuable educational experience for middle school, high school, and undergraduate science students in a variety of disciplines. We developed these modules so that they can be carried out with inexpensive equipment that may be readily available in many science classrooms. The module could potentially be further simplified, for example, using better insulation (e.g., a Styrofoam cooler) to avoid the need for close monitoring of temperatures or using custom-built approaches to gel electrophoresis (48). Furthermore, while 10-fold excess of staple strands is the standard approach, prior work has shown lower excess amounts, down to 5-fold excess reliably results in proper folding (24).

To date, either the extended or the condensed version of these experiments has been completed with middle and high school teachers at the 2019 Science Education Council of Ohio conference and at the 2018 Association for Biology Laboratory Education workshop. The condensed (∼1 h) experiment was also performed with middle school students at Hilltonia middle school. The full experiment has also been carried out in undergraduate classrooms both at Ohio State University in a mechanical engineering course (∼20 students) and by 2 different classes of systems and mechanical engineering students (∼50 students) at Otterbein University. Based on these experiences, we have found that students are generally successful. The most common prob-

Table 1. Required equipment and reagents.

Equipment		Reagents	
E1	Scale	**R1**	Distilled water
E2	Chemical Spoon	**R2**	$MgCl_2$
E3	Beakers	**R3**	GelGreen DNA stain
E4	Microwave	**R4**	Agarose
E5	Timer	**R5**	0.5x TBE
E6	Floating tube rack	**R6**	1 kb DNA ladder
E7	Graduated cylinder	**R7**	Loading Dye
E8	Hotplate	**R8**	Folding Reaction Buffer
E9	Thermometer	**R9**	M13mp18 DNA scaffold
E10	Gloves	**R10**	Horse oligos
E11	Calculator		
E12	Eppendorf tubes		
E13	Pipette and Tips		
E14	Gel Casting Equipment		
E15	Electrophoresis System		

lems we have encountered are incorrect use of pipettes, leading to incorrect volumes, and challenges loading folded samples into gels, leading to poking of the gel or not loading the full sample volume, but most students successfully fold structures and achieve the expected gel shifts.

This work is a foundation for implementing and translating DNA nanotechnology education with a hands-on approach to classrooms for undergraduate, secondary, and primary school students. Previous efforts translating DNA nanotechnology to undergraduate classrooms demonstrated DNA nanoswitches to introduce concepts of biosensing applications and conformational changes of DNA constructs (49). This work expands on this foundation by introducing the highly versatile and widely applicable DNA origami nanotechnology. We envision that this can achieve useful learning objectives (see Supplemental Table 2) and stimulate further opportunities to translate additional concepts and functions of DNA origami to classrooms, such as dynamic or complex DNA origami nanostructures and design and simulation modules. If design methods are introduced, students could even carry out design challenges, or design challenges could be carried out by assembling or applying existing structures, many of which are shared in an online database (50). Translating DNA origami nanotechnology into classrooms will play an important role in exposing young students to this highly promising cutting-edge approach that is likely to impact a wide range of industries that can educate students about potential fields and careers related to science, technology, engineering, and mathematics and reinforce other fundamental science and engineering learning milestones.

SUPPLEMENTAL MATERIAL

Supplemental files for this article are available at: https://doi.org/10.35459/tbp.2022.000228.S1.

AUTHOR CONTRIBUTIONS

All authors contributed to the Methods section of this research. PEB, AK, CEC, and MWH also analyzed the data, designed the figures, and wrote/reviewed the paper. CEC and MWH designed the teaching materials and performed the experiments in workshops, classrooms, and undergraduate laboratories.

DECLARATION OF INTERESTS

The authors declare no competing interests.

ACKNOWLEDGMENTS

This work was supported by start-up funding provided to MWH by Otterbein University and by NSF grant no. 1916740, 1921881, and 1351159 to CEC. We thank the Otterbein University Department of Engineering for purchasing the electrophoresis equipment used in the initial classroom implementations and to optimize protocols. We would also like to thank the Otterbein Engineering classes of 2019 and 2021 for testing the protocols and providing valuable feedback and members of the Castro Laboratory for providing useful feedback during development of the protocols. We would also like to acknowledge the Ohio State University (OSU) Pelotonia fellowship program for funding PEB. Transmission electron microscopy images were acquired at the OSU Campus Microscopy and Imaging Facility, which is supported in part by grant number P30 CA016058, National Cancer Institute, Bethesda, MD.

REFERENCES

1. Douglas, S. M., I. Bachelet, and G. M. Church. 2012. A logic-gated nanorobot for targeted transport of molecular payloads. *Science* 335:831–834. https://doi.org/10.1126/SCIENCE.1214081.
2. Li, S., Q. Jiang, S. Liu, Y. Zhang, Y. Tian, C. Song, J. Wang, Y. Zou, G. J. Anderson, J. Y. Han, Y. Change, Y. Liu, C. Zhang, L. Chen, G. Zhou, G. Nie, H. Yan, B. Ding, and Y. Zhao. 2018. A DNA nanorobot functions as a cancer therapeutic in response to a molecular trigger in vivo. *Nat Biotechnol* 36:258–264. https://doi.org/10.1038/nbt.4071.
3. Halley, P. D., C. R. Lucas, E. M. McWilliams, M. J. Webber, R. A. Patton, C. Kural, D. M. Lucas, J. C. Byrd, and C. E. Castro. 2016. Daunorubicin-loaded DNA origami nanostructures circumvent drug-resistance mechanisms in a leukemia model. *Small* 12:308–320. https://doi.org/10.1002/smll.201502118.
4. Veneziano, R., T. J. Moyer, M. B. Stone, E. C. Wamhoff, B. J. Read, S. Mukherjee, T. R. Sheperd, J. Das, W. R. Schief, D. J. Irvine, and M. Bathe. 2020. Role of

nanoscale antigen organization on B-cell activation probed using DNA origami. *Nat Nanotechnol* 15:716–723. https://doi.org/10.1038/s41565-020-0719-0.
5. Weiden, J., and M. M. C. Bastings. 2021. DNA origami nanostructures for controlled therapeutic drug delivery. *Curr Opin Colloid Interface Sci* 52:101411. https://doi.org/10.1016/j.cocis.2020.101411.
6. Rothemund, P. W. K. 2006. Folding DNA to create nanoscale shapes and patterns. *Nature* 440:297–302. https://doi.org/10.1038/nature04586.
7. Douglas, S. M., H. Dietz, T. Liedl, B. Högberg, F. Graf, and W. M. Shih. 2009. Self-assembly of DNA into nanoscale three-dimensional shapes. *Nature* 459:414–418. https://doi.org/10.1038/nature08016.
8. Dey, S., C. Fan, K. V. Gothelf, J. Li, C. Lin, L. Liu, N. Liu, M. A. D. Nijenhuis, B. Saccà, F. C. Simmel, H. Yan, and P. Zhan. 2021. DNA origami. *Nat Rev Methods Primers* 1:1–24. https://doi.org/10.1038/s43586-020-00009-8.
9. Zhou, L., A. E. Marras, H. J. Su, and C. E. Castro. 2014. DNA origami compliant nanostructures with tunable mechanical properties. *ACS Nano* 8:27–34. https://doi.org/10.1021/nn405408g.
10. Pfeifer, W., P. Lill, C. Gatsogiannis, and B. Saccà. 2018. Hierarchical assembly of DNA filaments with designer elastic properties. *ACS Nano* 12:44–55. https://doi.org/10.1021/acsnano.7b06012.
11. Nummelin, S., B. Shen, P. Piskunen, Q. Liu, M. A. Kostiainen, and V. Linko. 2020. Robotic DNA nanostructures. *ACS Synth Biol* 9:1923–1940. https://doi.org/10.1021/acssynbio.0c00235.
12. Blotnicky, K. A., T. Franz-Odendaal, F. French, and P. A. Joy. 2018. A study of the correlation between STEM career knowledge, mathematics self-efficacy, career interests, and career activities on the likelihood of pursuing a STEM career among middle school students. *Int J STEM Educ* 5:22. https://doi.org/10.1186/s40594-018-0118-3.
13. Castro, C. E., H. J. Su, A. E. Marras, L. Zhou, and J. Johnson. 2015. Mechanical design of DNA nanostructures. *Nanoscale* 7:5913–5921. https://doi.org/10.1039/C4NR07153K.
14. Martin, T. G., and H. Dietz. 2012. Magnesium-free self-assembly of multi-layer DNA objects. *Nat Commun* 3:1103. https://doi.org/10.1038/ncomms2095.
15. Shi, Z., and G. Arya. 2020. Free energy landscape of salt-actuated reconfigurable DNA nanodevices. *Nucleic Acids Res* 48:548–560. https://doi.org/10.1093/nar/gkz1137.
16. Wintersinger, C. M., D. Minev, A. Ershova, H. M. Sasaki, G. Gowri, J. F. Berengut, F. E. Corea-Dilbert, P. Yin, and W. M. Shih 2022. Multi-micron crisscross structures from combinatorially assembled DNA-origami slats. https://doi.org/10.1101/2022.01.06.475243 (preprint posted 7 January 2022).
17. Hudoba, M. W., Y. Luo, A. Zacharias, M. G. Poirier, and C. E. Castro. 2017. Dynamic DNA origami device for measuring compressive depletion forces. *ACS Nano* 11:6566–6573. https://doi.org/10.1021/acsnano.6b07097.
18. Wang, H., D. Luo, H. Wang, F. Wang, and X. Liu. 2021. Construction of smart stimuli-responsive DNA nanostructures for biomedical applications. *Chem Eur J* 27:3929–3943. https://doi.org/10.1002/chem.202003145.
19. Castro, C. E., F. Kilchherr, D. N. Kim, E. L. Shiao, T. Wauer, P. Wortmann, M. Bathe, and H. Dietz. 2011. A primer to scaffolded DNA origami. *Nat Methods* 8:221–229. https://doi.org/10.1038/nmeth.1570.
20. Majikes, J. M., and J. A. Liddle. 2021. DNA origami design: a how-to tutorial. *J Res Natl Inst Stan* 126:126001. https://doi.org/10.6028/jres.126.001.
21. Huang, C. M., A. Kucinic, J. A. Johnson, H. J. Su, and C. E. Castro. 2021. Integrated computer-aided engineering and design for DNA assemblies. *Nat Mater* 20:1264–1271. https://doi.org/10.1038/s41563-021-00978-5.
22. Nolan, T., and S. A. Bustin, editors. 2013. PCR Technology: Current Innovations. 3rd edition. CRC Press, Boca Raton, FL. https://doi.org/10.1201/b14930.
23. Wagenbauer, K. F., F. A. S. Engelhardt, E. Stahl, V. K. Hechtl, P. Stömmer, F. Seebacher, L. Meregalli, P. Ketterer, T. Gerling, and H. Dietz. 2017. How we make DNA origami. *Chem Bio Chem* 18:1873–1885. https://doi.org/10.1002/cbic.201700377.
24. Halley, P. D., R. A. Patton, A. Chowdhury, J. C. Byrd, and C. E. Castro. 2019. Low-cost, simple, and scalable self-assembly of DNA origami nanostructures. *Nano Res* 12:1207–1215. https://doi.org/10.1007/s12274-019-2384-x.
25. Seeman, N. C. 1982. Nucleic acid junctions and lattices. *J Theor Biol* 99:237–247. https://doi.org/10.1016/0022-5193(82)90002-9.
26. Watson, J. D., and F. H. C. Crick. 1953. Molecular structure of nucleic acids: a structure for deoxyribose nucleic acid. *Nature*. https://doi.org/10.1038/171737a0.
27. Elkin, L. O. 2003. Rosalind Franklin and the double helix. *Phys Today* 56:42–48. https://doi.org/10.1063/1.1570771.
28. Klug A. 1968. Rosalind Franklin and the Discovery of the Structure of DNA. *Nature* 219: 808–810. https://doi.org/10.1038/219808a0.
29. Liu, Y., and S. C. West. 2004. Happy Hollidays: 40th anniversary of the Holliday junction. *Nat Rev Mol Cell Biol* 5:937–944. https://doi.org/10.1038/nrm1502.
30. Holliday R. 1964. A mechanism for gene conversion in fungi. *Genet Res*5:282–304. https://doi.org/10.1017/S0016672300001233.
31. Zhang, F., S. Jiang, S. Wu, Y. Li, C. Mao, Y. Liu, and H. Yan. 2015. Complex wireframe DNA origami nanostructures with multi-arm junction vertices. *Nat Nanotechnol* 10:779–784. https://doi.org/10.1038/nnano.2015.162.
32. Veneziano, R., S. Ratanalert, K. Zhang, F. Zhang, H. Yan, W. Chiu, and M. Bathe. 2016. Designer nanoscale DNA assemblies programmed from the top down. *Science* 352:aaf4388. https://doi.org/10.1126/science.aaf4388.
33. Marras, A. E., L. Zhou, H. J. Su, and C. E. Castro. 2015. Programmable motion of DNA origami mechanisms. *Proc Natl Acad Sci* 112:713–718. https://doi.org/10.1073/pnas.1408869112.
34. List, J., E. Falgenhauer, E. Kopperger, G. Pardatscher, and F. C. Simmel. 2016. Long-range movement of large mechanically interlocked DNA nanostructures. *Nat Commun* 7:12414. https://doi.org/10.1038/ncomms12414.
35. Ketterer, P., E. M. Willner, and H. Dietz. 2016. Nanoscale rotary apparatus formed from tight-fitting 3D DNA components. *Sci Adv* 2. https://doi.org/10.1126/sciadv.1501209.
36. Shi, X., A. K. Pumm, J. Isensee, W. Zhao, D. Verschueren, A. Martin-Gonzalez, R. Golestanian, H. Dietz, and C. Dekker. 2022. Sustained unidirectional rotation of a self-organized DNA rotor on a nanopore. *Nat Phys* 18:1105–1111. https://doi.org/10.1038/s41567-022-01683-z.
37. Douglas, S. M., A. H. Marblestone, S. Teerapittayanon, A. Vazquez, G. M. Church, and W. M. Shih. 2009. Rapid prototyping of 3D DNA-origami shapes with caDNAno. *Nucleic Acids Res* 37:5001–5006. https://doi.org/10.1093/nar/gkp436.
38. Jun, H., F. Zhang, T. Shepherd, S. Ratanalert, X. Qi, H. Yan, and M. Bathe. 2019. Autonomously designed free-form 2D DNA origami. *Sci Adv* 5:eaav0655. https://doi.org/10.1126/sciadv.aav0655.
39. Matthies, M., N. P. Agarwal, and T. L. Schmidt. 2016. Design and synthesis of triangulated DNA origami trusses. *Nano Lett* 16:2108–2113. https://doi.org/10.1021/acs.nanolett.6b00381.
40. Benson, E., A. Mohammed, J. Gardell, S. Masich, E. Czeizler, P. Orponen, and B. Högberg. 2015. DNA rendering of polyhedral meshes at the nanoscale. *Nature* 523:441–444. https://doi.org/10.1038/nature14586.
41. Snodin, B. E. K., F. Randisi, M. Mosayebi, P. Šulc, J. S. Schreck, F. Romano, T. E. Ouldridge, T. Tsukanov, E. Nir, A. A. Louis, and J. P. K. Doye. 2015. Introducing improved structural properties and salt dependence into a coarse-grained model of DNA. *J Chem Phys* 142:234901. https://doi.org/10.1063/1.4921957.
42. Doye, J. P. K., T. E. Ouldridge, A. A. Louis, F. Romano, P. Šulc, C. Matek, B. E. K. Snodin, L. Rovigatti, J. S. Schreck, R. M. Harrison, and W. P. J. Smith. 2013. Coarse-graining DNA for simulations of DNA nanotechnology. *Phys Chem Phys* 15:20395–20414. https://doi.org/10.1039/C3CP53545B.
43. Maffeo, C., and A. Aksimentiev. 2020. MrDNA: a multi-resolution model for predicting the structure and dynamics of DNA systems. *Nucleic Acids Res* 48:5135–5146. https://doi.org/10.1093/nar/gkaa200.
44. Lee, J. Y., J. G. Lee, G. Yun, C. Lee, Y. J. Kim, K. S. Kim, T. H. Kim, and D. N. Kim. 2021. Rapid computational analysis of DNA origami assemblies at near-atomic resolution. *ACS Nano* 15:1002–1015. https://doi.org/10.1021/acsnano.0c07717.
45. Sobczak, J. P. J., T. G. Martin, T. Gerling, and H. Dietz. 2012. Rapid folding of DNA into nanoscale shapes at constant temperature. *Science* 338:1458–1461. https://doi.org/10.1126/science.1229919.
46. Kim, D. N., F. Kilchherr, H. Dietz, and M. Bathe. 2012. Quantitative prediction of 3D solution shape and flexibility of nucleic acid nanostructures. *Nucleic Acids Res* 40:2862–2868. https://doi.org/10.1093/nar/gkr1173.
47. Rumfelt, K. E., N. E. Wonderlin, D. Hulbert, and P. J. T. White. 2020. From DNA extraction to sequence analysis: a semester-long undergraduate research project on fish mislabeling. *Am Biol Teach* 82:170–175. https://doi.org/10.1525/abt.2020.82.3.170.
48. Ens, S., A. B. Olson, C. Dudley, N. D. Ross, A. A. Siddiqi, K. M. Umoh, and M. A. Schneegurt. 2012. Inexpensive and safe DNA gel electrophoresis using household materials. *Biochem Mol Biol Educ* 40:198–203. https://doi.org/10.1002/bmb.20596.
49. Abraham Punnoose, J., K. Halvorsen, and A. R. Chandrasekaran. 2020. DNA nanotechnology in the undergraduate laboratory: analysis of molecular topology using DNA nanoswitches. *J Chem Educ* 97:1448–1453. https://doi.org/10.1021/acs.jchemed.9b01185.
50. Poppleton, E., A. Mallya, S. Dey, J. Joseph, and P. Šulc. 2022. Nanobase.org: a repository for DNA and RNA nanostructures. *Nucleic Acids Res* 50:D246–D252. https://doi.org/10.1093/nar/gkab1000.